

Structural Relation Between the X-Phase and Other Phases in Ni_2MnGa

Tomoyuki Kakeshita¹, Takashi Fukuda^{1,a}, Tomoyuki Terai¹,
Toyotaka Osakabe² and Kazuhisa Kakurai²

¹Department of Materials Science and Engineering, Graduate School of Engineering,
Osaka University, 2-1, Yamada-oka, Suita, Osaka 565-0871, Japan

²Quantum Beam Science Directorate, Japan Atomic energy Agency,
Naka-gun, Ibaraki 319-1195, Japan

^afukuda@mat.eng.osaka-u.ac.jp

Keywords: incommensurate phase, critical phenomena, neutron diffraction, ferromagnetic shape memory alloy, nickel-manganese-gallium alloy

Abstract. We have investigated stress and temperature dependences of the structure of the X-phase in Ni_2MnGa to understand structural relation between the X-phase and other phases. Position and intensity of satellites of the X-phase are different from those of the intermediate (I-) phase under compressive stress, but they approach those of the I-phase with decreasing stress. That is, the structure change associated with the $\text{I} \rightarrow \text{X}$ transformation is discontinuous under a compressive stress, while it is continuous under zero stress. In addition, the transformation from the X-phase to the L2_1 -type parent phase is continuous regardless of applied stress. These results strongly suggest the existence of multi-critical point in Ni_2MnGa . On the other hand, the transformation from the X-phase to the martensite phase is discontinuous regardless of applied stress.

Introduction

Ferromagnetic shape memory alloy Ni_2MnGa exhibits a successive thermoelastic martensitic transformation. It has been widely accepted that the transformation sequence is a L2_1 -type parent phase (P-phase) to an intermediate phase (I-phase) and then to a martensite phase (M-phase) [1 - 4]. In addition to these phases, we recently found a new phase (X-phase) by compressive tests [5], and constructed a stress-temperature phase diagram [6]. According to the phase diagram, the X-phase exists even under zero stress. That is, transformation sequence of Ni_2MnGa under zero stress is $\text{P} \rightarrow \text{X} \rightarrow \text{I} \rightarrow \text{M}$, being different from the sequence reported before the finding of the X-phase. These results suggest that TA_2 phonon softening of the P-phase, which is so far considered to be one of the precursor phenomena of the $\text{P} \rightarrow \text{I}$ transformation [3, 4], is possibly related to the $\text{P} \rightarrow \text{X}$ transformation. Thus, the X-phase is important to understand the martensitic transformation in Ni_2MnGa .

Crystal structures of the M- and I-phases have been intensively investigated so far [7 -10], and recent studies suggest that they have incommensurate structures [12, 13]. Moreover, the X-phase also has an incommensurate structure according to our previous study [14]. Thus, three different incommensurate structures (M-, I- and X-phases) come to appear in Ni_2MnGa . Although these incommensurate structures are possibly related to each other, structural relation among P-, X-, I- and M-phases is not clear yet.

In the present study, therefore, we investigated structural relation among these phases by measuring stress and temperature dependences of satellite reflections of the X-, I- and M-phases in Ni_2MnGa .

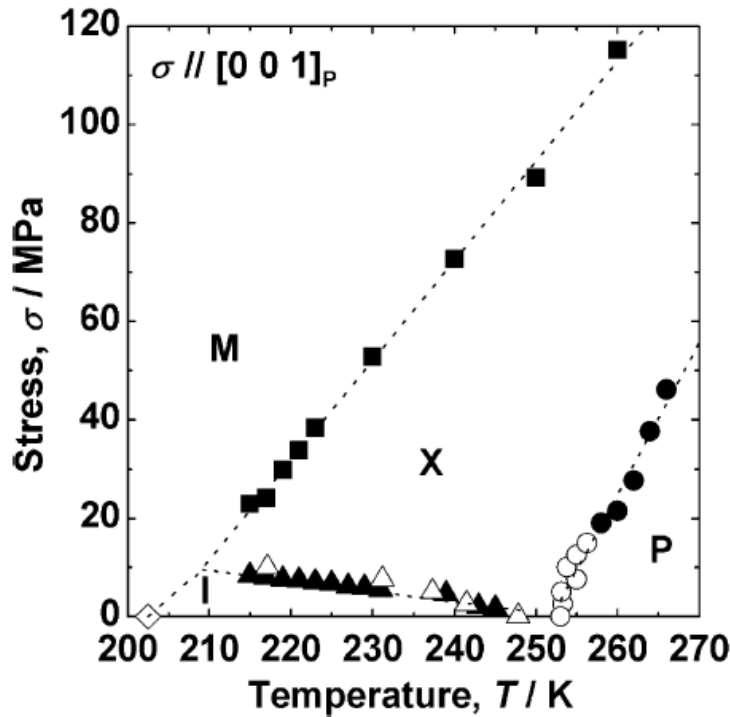


Fig. 1: Stress-temperature phase diagram of Ni_2MnGa obtained by applying compressive stress in the $[001]_P$ direction. (after [6])

Experimental Procedure

The specimen used in the present study is the same one used in the previous papers [13, 14]. An ingot of stoichiometric Ni_2MnGa was prepared by arc-melting, and a single crystal was grown from the ingot by a floating zone method. It was heat-treated at 1173 K for 24 h for homogenization and then at 923 K for 24 h to obtain a highly ordered L_{21} -type structure. A specimen with a dimension of $5.0 \times 1.9 \times 1.9 \text{ mm}^3$ and all edges being parallel to $\langle 001 \rangle_P$ was cut from the single crystal. The transformation temperature of the specimen was examined by a magnetic susceptibility measurement. The obtained transformation start temperatures are 259 K for the $P \rightarrow X$ transformation, 254 K for the $X \rightarrow I$ and 207 K for the $I \rightarrow M$. These temperatures are slightly higher than those of the specimen used to determine Fig. 1. So, the experimental conditions are determined taking the difference into consideration. Details of sample preparation are written elsewhere [13, 14].

Neutron diffraction measurements were made with a triple-axis spectrometer (TAS-1) using a non-polarized neutron beam at 2G beam-line of JRR-3 in Japan Atomic Energy Agency (JAEA). A wave length of 0.236 nm was selected through the neutron diffraction measurements. The horizontal collimation used was open-80'-80'-80'. A pyrolytic graphite filter was used to attenuate higher-order harmonic contaminations. Measurements were made in the temperature range of $190 \text{ K} \leq T \leq 260 \text{ K}$ under compressive stresses of $1 \text{ MPa} \leq \sigma \leq 100 \text{ MPa}$ applied in the $[001]_P$ direction by sweeping the scattering vector $\mathbf{q} = [h \ 2-h \ 0]^*_P$ in the range of $-0.1 \leq h \leq 2.1$. The lowest stress of the present experiment is about 1 MPa due to the weight of the piston used to apply external stress.

Results

Figure 2 shows stress dependence of neutron profile measured under different compressive stresses of $1 \text{ MPa} \leq \sigma \leq 100 \text{ MPa}$ at 255 K. In the case under 1 MPa, extremely weak satellite reflection appears at an incommensurate position of $h = 0.341$ (the index h represents the satellite position of $[h \ 2-h \ 0]^*_P$). Although this satellite is due to the X-phase, its position is close to that of the I-phase under zero stress reported in a previous paper [13]. The reason why satellites of the X- and I-phases appear at almost the same position is discussed later. We notice in Fig. 2 that the satellite position and intensity depend significantly on stress. That is, the position drastically moves from $h = 0.341$ (under 1 MPa) to $h = 0.369$ (under 50 MPa), and the intensity obviously increases with increasing stress. In addition to the position and intensity, full width at half maximum (FWHM) also depends on stress.

For example, the FWHM of the satellite reflection under 1 MPa is about 0.016, and that under 50 MPa is about 0.030. Such an increase in FWHM means that the variance of modulation wave length increases by the application of external stress. Incidentally, the profile under 100 MPa shows the coexistence of the X- and M-phases. This coexistence is due to the first-order nature of the stress-induced $X \rightarrow M$ transformation, being consistent with the stress-temperature phase diagram shown in Fig. 1.

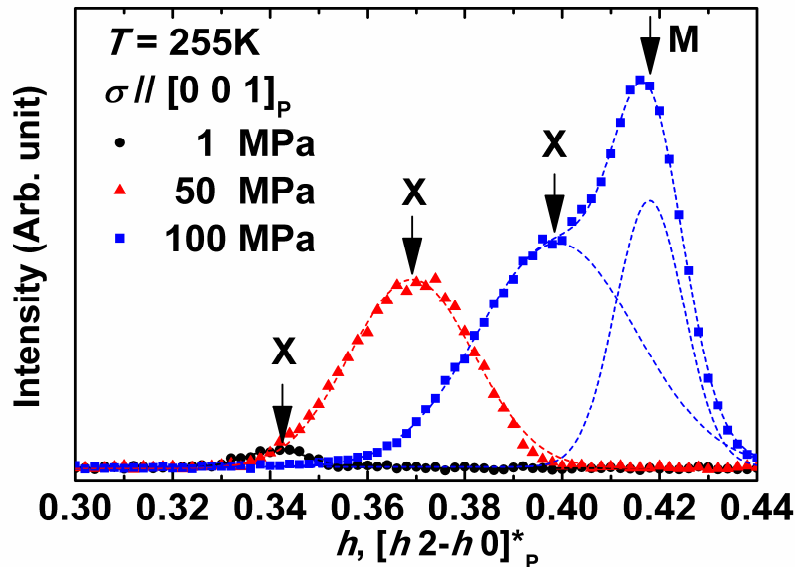


Fig. 2: Neutron diffraction profile of the X-phase at 255 K under different compressive stresses. The profile under 100 MPa comprises the X-phase and the M-phase.

Similar measurements have been made for the M-phase by fixing temperature at 190 K. The satellite reflection of the M-phase under 1 MPa appeared at $h = 0.426$, and it shifted to $h = 0.427$ under 25 MPa and to $h = 0.428$ under 40 MPa. While the satellite position depended slightly on the stress, satellite intensity and the FWHM (~ 0.016) kept almost the same values regardless of stress, meaning that the variance of modulation wave vector does not depend on stress in the M-phase.

By using the neutron profiles under various compressive stresses, we calculated lattice spacing d corresponding to $\{1\ 0\ 0\}_P$ planes of the X- and M-phases. The lattice spacing of the X-phase increased from 0.581 nm to 0.586 nm with increasing stress from 1 MPa to 85 MPa, while that of the M-phase kept almost the same value in the examined stress range. Using the stress dependence of the lattice spacing, the Young's modulus of the X-phase at 255 K is calculated to be about 4.8 GPa. In the calculation, we need Poisson's ratio of the X-phase, because d is measured perpendicular to applied stress. We assumed that the Poisson's ratio at 255 K is equal to that of the P-phase at 300 K, which is calculated to be 0.48 if we use the elastic constants reported by Worgull *et al.* [15]. The Young's modulus of the X-phase at 255 K is the same order as the value of the P-phase at 260 K, 7.0 GPa, obtained from initial slope of the stress-strain curve reported in the previous paper [6]. These low Young's moduli of the X- and P-phases possibly reflect lattice softening of the P- and X-phases near the $P \leftrightarrow X$ transformation temperature. This lattice softening was pointed out by Worgull *et al.* [15], although the X-phase was not recognized at that time.

Figure 3 shows temperature dependence of the neutron profile of the X-phase measured under a constant compressive stress of 10 MPa. In the case at 220 K, satellite reflection of the X-phase appears at an incommensurate position of $h = 0.361$. With increasing temperature, the satellite reflection obviously moves toward the nearest fundamental reflection of $[0\ 2\ 0]^*_P$, and its intensity drastically decreases. In addition to the change in position and intensity, the FWHM of the X-phase decreases from 0.024 at 220 K to 0.020 at 260 K.

Similar measurements have been made for the M-phase by fixing compressive stress to 1 MPa. Satellite reflection of the M-phase at 190 K appeared at an incommensurate position of $h = 0.427$, and slightly moves to $h = 0.426$ at 200 K and then to $h = 0.424$ at 210 K. In addition, the intensity slightly

decreased with increasing temperature. The FWHM kept almost the same value of 0.016 regardless of temperature, which resembles the stress dependence of the FWHM described above.

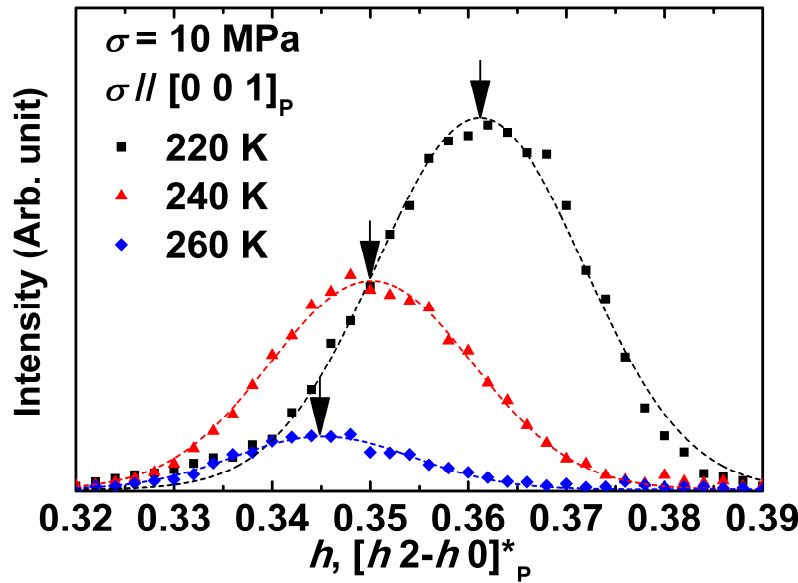


Fig. 3: Neutron diffraction profiles of the X-phase under compressive stress of 10 MPa at different temperature.

Discussion

In the previous section, we described the stress and temperature dependences of satellite reflections of the X- and M-phases. The obtained results of satellite positions of the X- and M-phases are summarized in Fig. 4 together with those of the I-phase under zero stress reported in the previous paper [12]. In the followings, we will discuss the structural relation between the X-phase and the other phases by referring Fig. 4.

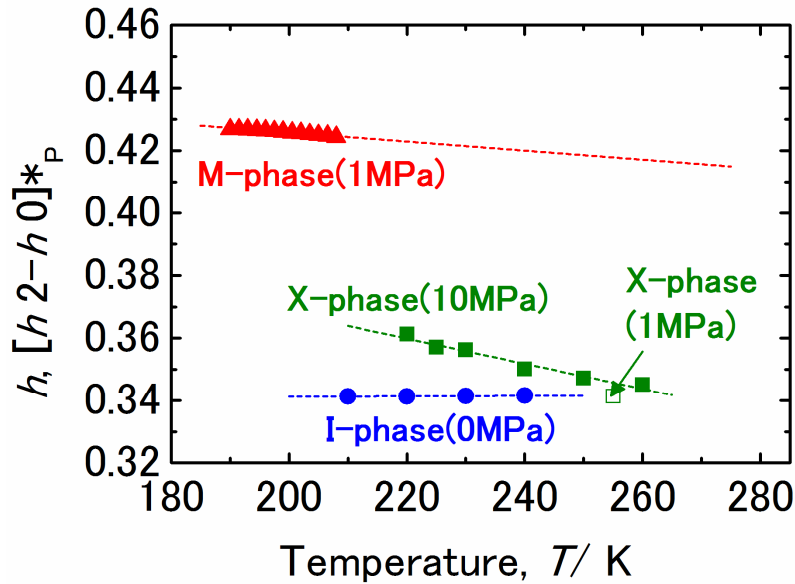


Fig. 4: Temperature dependences of satellite position in Ni_2MnGa .

First, we discuss the structural relation between the X- and M-phases. It is seen in Fig. 4 that the satellite position of the X-phase are obviously different from those of the M-phase for all the temperature region examined in the present study. In addition, the FWHM of the X-phase is nearly twice that of the M-phase as seen in Fig. 2. Consequently, the $X \rightarrow M$ transformation is a first-order one regardless of temperature. The existence of stress hysteresis in the stress-strain curves associated with the $X \rightarrow M$ transformation [5, 6] also support the above interpretation.

Second, we discuss the structure relation between the X- and P-phases. A transmission electron microscope observation of the present alloy showed that satellite position and intensity of the X-phase are almost the same as those of the P-phase in the vicinity of the $X \rightarrow P$ transformation temperature [16]. This result suggests that the $X \rightarrow P$ transformation is a second-order-like one. No stress hysteresis in the stress-strain curves and no temperature hysteresis in the magnetic susceptibility curves associated with the $P \leftrightarrow X$ transformation [5, 6] also support the above interpretation.

Finally, we discuss the structure relation between the X- and I-phases. Except for in the vicinity of the $I \rightarrow X$ transformation temperature under zero stress, $T_0^{I \rightarrow X}$, the $I \rightarrow X$ transformation is a first-order one. This is because the I- and X-phases coexist in association with the transformation and a hysteresis exists for the transformation [6, 14]. In the vicinity of $T_0^{I \rightarrow X}$, however, the transformation is continuous as seen in Fig. 4. That is, the satellite position of the X-phase approaches that of the I-phase on approaching $T_0^{I \rightarrow X}$. In addition, the intensity of the I-phase at zero stress approaches that of the X-phase at 1 MPa on approaching $T_0^{I \rightarrow X}$. Therefore, the satellite reflection of the X-phase under zero stress is indistinguishable from that of the I-phase. This is the reason why the X-phase, which exists even under zero stress, has not been found by means of neutron, X-ray and electron diffraction experiments reported so far.

From the above results, it is most likely that Ni_2MnGa has a multi-critical point like the one observed in SrTiO_3 [17]. That is, second-order-like $P \rightarrow X$ transformation is followed by second-order-like $X \rightarrow I$ transformation and these two transformations occur almost at the same temperature.

Conclusions

Stress and temperature dependences of the structure of the X-phase in Ni_2MnGa have been investigated by neutron diffraction measurements under compressive stress in order to clarify structural relation among the P-, I-, M- and X-phases. The structure of the X-phase in Ni_2MnGa depends strongly on stress and temperature compared with that of the M-phase and/or the I-phase. In association with the $X \rightarrow M$ transformation, both the position and intensity of the satellite reflection changes drastically regardless of stress and temperature. In association with the $X \rightarrow P$ transformation, the intensity of the satellite reflection fades gradually. In association with the $I \rightarrow X$ transformation, the position and intensity of the satellite changes drastically when the transformation occur under compressive stress, while they changes continuously when it occurs under zero stress.

Acknowledgements

This study was supported by The Global COE Program (Project: Center of Excellence for Advanced Structural and Functional Materials Design) from MEXT, Japan. This work was performed under the Common-Use Facility Program of JAEA.

References

- [1] P. J. Webster, K. R. A. Ziebeck, S. L. Town and M. S. Peak: *Phil. Mag. B* Vol. 49 (1984), p.295

-
- [2] V. V. Kokorin, V. A. Chernenko, E. Cesari, J. Pons and C. Segui, *J. Phys.: Condens. Matter*: Vol. 8 6457 (1996), p. 6457
- [3] A. Zheludev, S. M. Shapiro, P. Wochner, A. Schwartz, M. Wall and L. E. Tanner: *Phys. Rev. B* Vol. 51 (1995), p. 11310
- [4] A. Planes, E. Obradó, A. G. Comas and L. Manósa: *Phys. Rev. Lett* Vol. 79 (1997), p. 3926
- [5] J. H. Kim, T. Fukuda and T. Kakeshita: *Scripta Mater.* Vol. 54 (2006), p. 585
- [6] H. Kushida, K. Hata, T. Fukuda, T. Terai and T. Kakeshita: *Scripta Mater.* Vol. 60 (2009), p. 96
- [7] V. V. Martynov and V. V. Kokorin: *J. Phys. (France) III* 2, (1992), p.739
- [8] A. Zheludev, S. M. Shapiro, P. Wochner and L. E. Tanner: *Phys. Rev. B* Vol. 54 (1996), p. 15045.
- [9] J. Pons, V. A. Chernenko, R. Santamarta and E. Cesari: *Acta Mater.* Vol. 48 (2000), p. 3027
- [10] P. J. Brown, J. Creangle, T. Kanomata, M. Matsumoto, K. U. Neumann, B. Ouladdiaf and K. R. A. Ziebeck: *J. Phys.: Condens. Matter* Vol. 14 (2002), p. 10159
- [11] T. Ohba, N. Miyamoto, K. Fukuda, T. Fukuda, T. Kakeshita and K. Kato: *Smart Mater. Struct.* Vol. 14 (2005) p. S197
- [12] L. Righi, F. Albertini, L. Pareti, A. Paoluzi and G. Calestani: *Acta Mater.* Vol. 55 (2007), p. 5237
- [13] H. Kushida, K. Fukuda, T. Terai, T. Fukuda, T. Kakeshita, T. Ohba, T. Osakabe, K. Kakurai and K. Kato, *Eur. Phys. J. Special Topics*, Vol. 158 (2008), p. 87
- [14] H. Kushida, T. Terai, T. Fukuda, T. Kakeshita, T. Osakabe and K. Kakurai: *Scripta Mater.* Vol. 60 (2009), p. 248
- [15] J. Worgull, E. Petti and J. Trivisonno: *Phys. Rev. B* Vol. 54 (1996), p.15695
- [16] T. Fukuda, H. Kushida, M. Todai, T. Kakeshita and H. Mori: *Scripta Mater.* DOI: 10.1016/j.scriptamat.2009.04.046
- [17] K. A. Müller, W. Berlinger and J. C. Slonczewski, *Phys. Rev. Lett.*, Vol. 25 (1970), p. 734